NASA TM X-62,295

NASA TECHNICAL
MEMORANDUM

NASA TM X-62,295

RATES AND MECHANISMS OF THE ATOMIC OXYGEN REACTION WITH NICKEL AT ELEVATED TEMPERATURES

Jerry D. Christian and William P. Gilbreath

Ames Research Center
Moffett Field, Calif. 94035

August 1973

RATES AND MECHANISMS OF THE ATOMIC OXYGEN REACTION WITH NICKEL AT ELEVATED TEMPERATURES

Jerry D. Christian* and William P. Gilbreath

Ames Research Center, NASA, Moffett Field, Calif., 94035

ABSTRACT

The oxidation of nickel by atomic oxygen at pressures from 1 to 45 Nm^{-2} between 1050 and 1250°K has been investigated. In these ranges, the oxidation was found to follow the parabolic rate law, viz., $k_p = 1.14 \times 10^{-5} \exp(-13410/T)\ g^2 cm^{-4}\ sec^{-1}$ for films of greater than 1 μm thickness and was pressure independent. The activation enthalpy for the oxidation reaction was 112 ±11 kJ $mole^{-1}$ (27 ±3 kcal $mole^{-1}$). Of a number of possible mechanisms and defect structures considered, it was shown that the most likely was a saturated surface defect model for atomic oxidation, based on reaction activation enthalpies, impurity effects, pressure independence, and magnitudes of the rates. A model judged somewhat less likely was one having doubly ionized cationic defects rate controlling in both atomic and molecular oxygen. From comparisons of the appropriate processes, the following enthalpy values were derived: ΔH^* (Ni diffusion in NiO) = 110 ±30 kJ $mole^{-1}$ and ΔH_f^o (doubly ionized cation vacancies in NiO from atomic oxygen) = −9 ±25 kJ $mole^{-1}$.

*NRC Senior Postdoctoral Resident Research Associate.

Page Intentionally Left Blank

SYMBOLS

C, C', C"	collective constants
D	diffusion coefficient
(d)	doubly ionized vacancy
ΔG^{o}	standard free energy of formation
ΔH^{o}	standard enthalpy change for reaction
ΔH^{*}	enthalpy of activation
K	equilibrium constant
k, k'	rate constant
(n)	non-ionized vacancy
P	pressure
R	gas constant
ΔS^{o}	standard entropy change for reaction
(s)	singly ionized vacancy
(s → d)	singly to doubly ionized vacancy reaction
T	absolute temperature
t	time
w	weight
x	thickness
y	defect mole fraction
[ ]	concentration
□	vacancy

Subscripts

a, c	refer to reactions (a) and (c), respectively
diff	vacancy diffusion

f	formation
Ni,O,O_2	refers to process or constant involving particular element
o	initial state
p	parabolic
σ	conductance

RATES AND MECHANISMS OF THE ATOMIC OXYGEN REACTION WITH NICKEL AT ELEVATED TEMPERATURES

Jerry D. Christian* and William P. Gilbreath

Ames Research Center, NASA, Moffett Field, Calif., 94035

The oxidation rates of nickel and the defect structure and transport properties of nickel oxide in molecular oxygen have been the subjects of numerous investigations. It is generally agreed that NiO is a p-type, metal-deficient, semiconductor and that the transport and growth properties of NiO on nickel are controlled by cationic diffusion of nickel through the NiO lattice in the presence of nickel ion vacancies created at the gas-oxide interface.[1-5] At present, however, there is considerable controversy as to whether the cation vacancies in NiO are predominantly singly ionized[2,4,6,7] or doubly ionized[1,4,8-10] under ordinary conditions of pressure and in the temperature range of about 800 to 1700°K. Furthermore, experimental values of activation energies for the various kinetic and transport processes are not all in accord.

No systematic study has been performed on the effect of dissociated oxygen on the magnitude of the oxidation rate of nickel and on the activation energy for this process. Nickel is the base metal in many high-temperature alloys for which dissociated gas exposure may occur in service. We have therefore measured the rates of reaction of nickel with atomic oxygen and, by comparing the results with those for the molecular oxygen reaction, have developed a model for the mechanism of the process.

EXPERIMENTAL

The sample was suspended from an Ainsworth Type 14 recording semimicrobalance (10 μg sensitivity) in a vacuum system and the amount of oxidation per unit time was determined from the weight increase. A small bifilar wound furnace was placed around the sample inside the vacuum system and was, in turn, surrounded by a 5-cm-diameter quartz tube connected to the metal vacuum system by means of a quick disconnect O-ring fitting. Figure 1 is a photograph of the furnace. The core and outer radiation shield were fabricated from boron nitride. The grooved core was wrapped snugly with 0.38-mm (15 mil) diameter Pt-13% Rh wire at eight turns per centimeter (four turns per centimeter in each direction) and then coated with a ceramic adhesive to improve the thermal contact between the wire and the core. The total room temperature resistance of the windings was 6.7 Ω. The steady-state temperature (in vacuum) is plotted as a function of applied power in figure 2. At an inside furnace temperature of 1475°K, the winding temperature was 1550°K. The middle 1.5-cm section of the furnace was uniform to about 5° at 1175°K. (The sample length was 1.2-cm.)

*NRC Senior Postdoctoral Resident Research Associate.

The nickel samples were mechanically cleaned by abrasion with 500-grit silicon carbide polishing paper, wiped clean, and washed two cycles with water, carbon tetrachloride, and isopropyl alcohol. A specimen was vacuum annealed at the beginning temperature of a series of measurements. An initial oxidation was allowed to occur until the oxide skin exceeded 1000 nm (see Results). This ensured also that residual organic surface contaminants were no longer present. Subsequent oxidation rate measurements were made on a single sample at several different temperatures, usually with cooling between runs. As detailed in table I, oxidation experiments were conducted on nickel specimens

TABLE I.– IMPURITY ANALYSIS OF NICKEL SPECIMENS

Element	Concentration (ppm)		Element	Concentration	
	Material 1*	Material 2**		Material 1*	Material 2**
Ag	0.25		N		3
Al	31		Na	0.26	
As	5.9		Nb	0.53	
B	15		O		18
C	(Not reported)	37	P	<1	
Ca	1.8		Pb	9.1	
Cd	<1		S	45	
Cl	2.7		Sb	5.9	
Co	1500		Si	650	
Cr	290	2	Sn	1.1	3
Cu	3400		Ta	1.2	
Fe	2500	12	Ti	360	
Ga	1.7		Th	<1	
Ge	0.4		V	7	
Hf	2		W	10	
K	1.3		Zn	1.1	
Mg	400		Zr	0.82	
Mn	6500		Ni	98.4%	99.99+%
Mo	37				

*All elements not reported, <0.1 ppm.
***All elements not reported, <1 ppm.

of two different purities. Spark source mass spectroscopic analysis was used to determine the impurity level in the less pure material while the vendor (Alfa Inorganics) supplied the analysis on the other. The effect of the various impurities on the results is considered in the Discussion.

Oxygen was flowed through the apparatus at a linear flow velocity in the range of 40 to 1500 cm sec^{-1}. A microwave cavity of foreshortened 1/4 wave coaxial electrical configuration with resonance frequency adjustment (similar to cavity 5 of Fehsenfeld et al.[11] but modified to accommodate a 5-cm-diameter tube) was placed around the quartz tube and positioned at the center of the furnace and sample. It was attached via a waveguide to a Raytheon PGM 2450 MHz microwave power supply (100 W maximum) which had been modified[12] to improve

its stability to 0.1%. With the microwave power supply on, a discharge was initiated in the flowing O_2 with a Tesla coil. A stable discharge, which partially dissociated the O_2, could be maintained in the total pressure range of 1 to 50 Nm^{-2} (0.01 to 0.4 Torr).

The discharge, as well as the flowing gas, affected the balance readings slightly but, as we were interested only in changes of weight, the constant extraneous deflections cancelled out.

The furnace temperature was allowed to reach steady state with the sample suspended in vacuo and then O_2 flow was started and the discharge begun.

The temperature was measured by a calibrated Pt-10%Rh thermocouple placed near the sample. The thermocouple junction was covered with a boron nitride cap to protect it from the effects of recombining atomic oxygen. Its temperature readings were calibrated to those of the sample by comparing its readings with those of a 0.25-mm (10-mil) thermocouple imbedded in the sample in a series of temperature calibration experiments. The true temperature of the sample was obtained by turning off the microwave power supply and extrapolating the recorded temperature back to the instant of power turnoff. In this way, extraneous voltages resulting from the microwave field and discharge were eliminated. In some later experiments, 25-μm (1-mil) lead wires were attached to a 0.25-mm thermocouple imbedded in the sample and annealed. The sample temperature was measured, as described above, directly following the weight change measurements.

The partial pressure of O was determined by titrating with NO_2 at the end of an experiment according to the method of Kaufman.[13-15] In this method, the fast reaction

$$NO_2 + O \rightarrow NO + O_2$$

is followed by the light-emitting slow reaction:

$$NO + O \rightarrow NO_2 + h\nu$$

which is used as an indicator for the first reaction. Accordingly, the light output reaches a maximum when the NO_2 flow rate is half that of the O flow rate and then falls symmetrically to zero at the endpoint at which the NO_2 flow equals the O flow.

The O_2 flow rate was determined by measuring, near atmospheric pressure, the pressure drop across a capillary with a differential manometer[16] filled with H_2O. The manometer had been calibrated by observing the flow rate through a burette using soap bubbles at a known temperature and pressure. Gas pressure at the supply tank was regulated to just above ambient pressure by a sensitive, 5-psig, regulator (Matheson Model No. 70) and, following the flow-measuring apparatus, was reduced to the system pressure by means of a very fine needle valve.

Nitrogen dioxide flow rates were determined by observing the pressure, as a function of time, in a storage vessel of known volume (about 2 liters at an initial pressure of approximately 1.5×10^4 Nm^{-2}) and the temperature as the gas was introduced to the system through a needle valve. Flow rates were corrected for the amount of association to N_2O_4 calculated for the average pressure of a given flow rate measurement.

Light intensity measurements were made downstream from NO_2 introduction with an RCA 1P21 photomultiplier equipped with a Corning CS3-72 light filter. This combination gave the best filtering of ambient light and good response to the emitted light. In practice, we found that the endpoint could be conveniently detected visually in a darkened room just as accurately as by plotting the photomultiplier output vs. flow rate.

The fraction of O_2 dissociation determined by this method was multiplied by twice the O_2 pressure, measured prior to turning on the discharge, to obtain the partial pressure of O.

We obtained very large fractions of dissociation of O_2, up to 50%. The flow rate was found to be the most important parameter in the control of percent dissociation of the O_2. The effects of flow rate, pressure, microwave power, and temperature on the percent dissociation of O_2 are shown in figures 3, 4, 5, and 6. The introduction of a metal sample had only a slight effect on the measured concentration of atomic oxygen. We could control the presence or absence of a "tail" in the discharge in the flowing gases below the furnace and its presence increased the amount of dissociation by a factor of 1.6.

The point of introduction of the NO_2, whether made adjacent to the sample inside the furnace or above (downstream from) the discharge zone, had no effect on the measured atom concentrations at room temperature and 10 Nm^{-2} O (35% dissociation). However, at 1160°K, the measured quantity outside the discharge zone was 25% smaller than inside the discharge zone under conditions of $P_O \sim 1$ Nm^{-2} (0.01 Torr) at 4% dissociation.

RESULTS

Past investigators[17-24] of nickel oxidation have shown that a growth rate transition occurs at oxide thicknesses of 100 to 1000 nm. At greater thicknesses, the rate of growth of the oxide is generally found to be inversely proportional to its thickness, x, that is,

$$\frac{dx}{dt} = \frac{k'_p}{x}$$

In integrated form, then,

$$x^2 = x_o^2 + 2k'_p t$$

or

$$w^2 = w_o^2 + k_p t$$

where $w - w_o$ is the total weight increase from $t_o = 0$. This parabolic rate law has been interpreted in terms of the concentration of nickel ion vacancies formed at the gas-oxide interface controlling the diffusion rate of cations from the metal-oxide interface to the gas-oxide surface.[25-27] Our measurements in atomic oxygen were all done with oxide film thicknesses greater than 1000 nm, and the results were found to follow the parabolic rate law. Values of the parabolic rate constants for atomic oxygen were calculated from the total rate data by applying small corrections (<5%) for molecular oxygen contributions. An Arrhenius plot of the atomic oxygen parabolic rate constants for nickel is shown in figure 7 for the two materials examined. The data were obtained in partial pressures of atomic oxygen varying from 1 to 40 Nm^{-2} (0.01 to 0.3 Torr). The parabolic rate constants were independent of atomic oxygen partial pressure in this range (see Discussion). For comparison, the data of Douglass et al.[28] for air reaction at ambient pressure with nickel, which may be taken as representative of molecular oxygen results, were extrapolated to 7 Nm^{-2} on the basis of a $P_{O_2}^{1/6}$ dependence (as discussed later) and are also shown in the figure. The only prior work with the Ni-atomic oxygen system was by Dickens et al.,[29] who measured the rates at two much lower temperatures and at much smaller reported partial pressures (1 mN m^{-2} compared to the present 10 Nm^{-2}).[a] Their data are included in figure 7; the linear least-squares fit to our data for material, for which the most complete and precise results were obtained ($\ln k_p = -11.38 - 13410/T$; k_p in $g^2cm^{-4}sec^{-1}$) extrapolated to their temperatures shows good agreement between the two investigations.

A value of 27 kcal $mole^{-1}$ is obtained from the slope of log k_p vs. T^{-1} for atomic oxygen reaction with nickel.[b] Based on the standard error of estimate, we estimate the error range to be ±3 kcal $mole^{-1}$.

---

[a]These authors estimated their partial pressures on the assumption that enhanced atom recombination at the higher temperatures of their experiments decreased the atom concentration by as much as a factor of 600 from the value they measured at room temperature. However, in our apparatus, we observed little effect of temperature on the percent dissociation of O_2. It is possible, therefore, that the partial pressures of Dickens et al. may be as high as 100 times their reported values. This is, however, difficult to assess accurately because we continuously created the atoms in the furnace zone while Dickens dissociated the oxygen upstream of their furnace and sample.

[b]To facilitate comparisons of the present work with numerous previous studies, calories are used as the unit of heat and energy (1 calorie = 4.184 Joules).

DISCUSSION
Role of Vacancies in Nickel Oxidation

The parabolic corrosion rate of nickel in molecular oxygen is considered to be controlled by the diffusion rate of nickel ions through the NiO lattice, which, in turn, is proportional to the concentration gradient of the cation vacancies between the gas-oxide interface and the metal-oxide interface. Vacancies are created by a series of reactions which may be represented by the net equations:

$$Ni^{2+} + 1/2\ O_2 = O^{2-} + Ni^{3+} + Ni\square^{+} \qquad (a)$$

$$Ni\square^{+} + Ni^{2+} = Ni^{3+} + Ni\square \qquad (b)$$

$$2Ni^{2+} + 1/2\ O_2 = 2Ni^{3+} + Ni\square + O^{2-} \qquad (c)$$

The charged species represent ions in the NiO lattice. $Ni\square^{+}$ and $Ni\square$ represent singly ionized and doubly ionized vacancies for Ni^{2+}. It has been established[30,31] that non-ionized vacancies, $Ni\square^{++}$, are not significant as defects. Because of the small dissociation pressure of NiO, the vacancy defect concentration formed at the metal-oxide interface is practically zero and thus the vacancy concentration gradient in the oxide lattice between the metal-oxide and oxide-gas interfaces can be taken as equal to the vacancy concentration at the gas-oxide surface.

By a variety of methods, investigators have attempted to determine whether reaction (a) or reaction (c) predominates under the conditions of their experiments. By applying the mass action law and noting that, for reaction (a), $[Ni^{3+}] = [Ni\square^{+}]$ (when reaction (b) occurs insignificantly), or, for reaction (c), $[Ni^{3+}] = [2Ni\square]$ (when doubly ionized vacancies predominate), one can show that, for conditions where an equilibrium concentration of vacancy defects exists, for predominately singly ionized vacancies,

$$[Ni\square^{+}] = K_a^{1/2} P_{O_2}^{1/4} = P_{O_2}^{1/4} \exp\left[\frac{-\Delta H_a^o}{2RT} + \frac{\Delta S_a^o}{2R}\right] = C_a P_{O_2}^{1/4} \exp\left[\frac{-\Delta H_a^o}{2RT}\right] \qquad (1)$$

or, for the case of doubly ionized vacancies predominating,

$$[Ni\square] = 4^{-1/3} K_c^{1/3} P_{O_2}^{1/6} = 4^{-1/3} P_{O_2}^{1/6} \exp\left[\frac{-\Delta H_c^o}{3RT} + \frac{\Delta S_c^o}{3R}\right] = C_c P_{O_2}^{1/6} \exp\left[-\frac{\Delta H_c^o}{3RT}\right] \qquad (2)$$

Mole fractions are used for concentrations and $[Ni^{2+}] \approx [O^{2-}] \approx 1$ when the defect concentrations are small. Note that reaction (a) should produce a $P_{O_2}^{1/4}$ dependence for the equilibrium vacancy concentrations, while a $P_{O_2}^{1/6}$ dependence is expected for predominately doubly ionized vacancies (reaction (c)).

Many investigations (e.g., refs. 1, 2, 4, 6-10), both experimental and theoretical, have been performed to detect or predict the relative amounts of the two types of cation vacancies in NiO — unfortunately, conclusions from these works can support the predominance of either type. In balance, however, one factor gives more credence to those proponents of the doubly ionized vacancies. Aliovalent impurities in nickel are predominately of valence greater than 2, which would tend to increase the pressure dependence of vacancy-related properties.[32] And since, even in high purity nickel, the impurity concentration is of the same magnitude as the defect concentration,[8,32] those higher pressure dependence results, i.e., $P^{1/4}$, could arise from an impurity effect.

Reaction Enthalpies in Nickel Oxidation

In the following discussion, with the aid of the results from the present investigation in atomic oxygen, a detailed examination will be made of the various types of cation vacancies which can be present in NiO and control the oxidation behavior.

If the rate of reaction of Ni with O_2 is proportional to the diffusion rate of nickel ions in the oxide layer, which in turn is proportional to the cationic vacancy concentration formed at the gas/oxide interface, then

$$\text{Rate } O_2 = C''[\text{Ni}\square] \cdot D_{\text{Ni}} = C''[\text{Ni}\square]D_o \exp(-\Delta H^*_{\text{diff}}/RT)$$

for doubly ionized vacancies. If the vacancy defect concentration is the equilibrium value at all temperatures of measurement, then substituting equation (2) for $[\text{Ni}\square]$:

$$\text{Rate } O_2 = C''C_c D_o P_{O_2}^{1/6} \exp\left[\frac{\left(1/3\Delta H^o_f(d) + \Delta H^*_{\text{diff}}\right)}{RT}\right]$$

D_{Ni} is the diffusion coefficient of nickel ion vacancies through NiO (or of Ni vacancies, an equivalent process); C", D_o and C_c are constants; ΔH^*_{diff} is the net activation enthalpy for Ni diffusing via vacancies in NiO; and $\Delta H^o_f(d) = \Delta H^o_c$ is the thermodynamic standard enthalpy of formation of doubly ionized vacancies from O_2, i.e., the standard enthalpy change for reaction (c). (d and s are used following ΔH^o_f to indicate doubly and singly ionized vacancies, respectively.)

Furthermore,

$$\text{Rate } O_2 = C' \cdot \exp\left[\frac{-\Delta H^*_{O_2}}{RT}\right]$$

where $\Delta H^*_{O_2}$ is the measured activation enthalpy for reaction of Ni with O_2. Thus,

$$\Delta H^*_{O_2} = \Delta H^*_{diff} + 1/3\,\Delta H^o_f\,(d) \qquad (3)$$

Similarly, if one assumes that singly ionized vacancies are instead the important defects, the following expression can be derived:

$$\Delta H^*_{O_2} = \Delta H^*_{diff} + 1/2\,\Delta H^o_f\,(s) \qquad (4)$$

As developed below, ΔH^*_{diff} may be calculated from experimental values for the other terms in equations (3) and (4).

$\Delta H^o_f(y)$ has been determined by several means as tabulated in table II. As shown, $\Delta H^o_f(y)$ calculated from diffusion data, using the equation given by Mitoff,[8] is considerably lower (and, in one case, negative) than the other values.

TABLE II.— ENTHALPY OF VACANCY FORMATION IN NiO

$\Delta H^o_f(y)$, kcal mole^{-1}	Method	Reference
19.8	Gravimetric	32
24 ±8	Gravimetric	8
17.8 ±3	Electrical conductivity	8
11.4*	Diffusion	8 from 33, 34
5.4*	Diffusion	calc. from 35
-6.4*	Diffusion	calc. from 36
19.1 ±0.7	Electrical conductivity	10
19	Electrical conductivity	37
19.5 ±2	Weighted mean (neglecting * values)	

The mean (19.5 ±2 kcal mole^{-1}, which neglects the diffusion results and is weighted according to the precision of the others) is apparently well representative of $\Delta H^o_f(y)$. This is also consistent with the observations of Koel and Gellings[30] who report a value of 20 kcal mole^{-1} for 1/2 $\Delta H^o_f(s)$ and 21.7 kcal mole^{-1} for 1/3 $\Delta H^o_f(d)$. (If the vacancies are doubly ionized, then 1/3 $\Delta H^o_f(d) = \Delta H^o_f(y)$ and, if they are singly ionized, 1/2 $\Delta H^o_f(s) = \Delta H^o_f(y)$.)

Reported values for the activation enthalpy for nickel oxidation by molecular oxygen, $\Delta H^*_{O_2}$, ranges[4,19,28,38-45] from 38 to 68 kcal mole^{-1}. An average of all results is 46 ±6 kcal mole^{-1}.

By substituting the values $\Delta H^*_{O_2}$ = 46 ±6 kcal mole^{-1} and 1/3 $\Delta H^o_f(d)$ = (19.5 ±2) kcal mole^{-1} or 1/2 $\Delta H^o_f(s)$ = (19.5 ±2) kcal mole^{-1} into equation (3) or (4), respectively, one obtains a calculated value[c] of ΔH^*_{diff} of (26.5 ±7) kcal mole^{-1}. This value is used in later calculations.

[c]Recently, Koel and Gellings[30] reported an experimentally determined value of 24.6 kcal mole^{-1} for this quantity. In view of the close agreement with the calculated value, the error ranges given for ΔH^*_{diff} and $\Delta H^*_{O_2}$ are probably overestimated.

Development of Vacancy Models

We now consider the theoretical relationships between O_2 activation enthalpies and O activation enthalpies for reaction with nickel for the various possible combinations of equilibrium vacancy situations where only one type of vacancy exists in each environment. These are (1) singly ionized vacancies in both cases, (2) doubly ionized vacancies in both cases, (3) doubly ionized vacancies in O_2 and singly ionized vacancies in O, (4) singly ionized vacancies in O_2 and doubly ionized vacancies in O, (5) doubly ionized vacancies in O_2 and non-ionized vacancies in O, and (6) singly ionized vacancies in O_2 and non-ionized vacancies in O. Non-ionized vacancies in O_2 have been demonstrated[30] not to be important. This is also demonstrated by the fact that electrical conductivity measurements have shown NiO in O_2 to be a p-type conductor in which positive holes (Ni^{3+}) are formed which requires formation of ionized vacancies.[8] A seventh situation is possible in O — the vacancy concentrations (for any degree of ionization) are constant at the same value for all pressures and temperatures investigated.

Equations are tabulated below with the respective ΔH^o symbols and relationships following each for the six different equilibrium cases. O_2 or O have been added to the symbols for $\Delta H_f^o(d)$ and $\Delta H_f^o(s)$ to distinguish between formation from O_2 or O, respectively; n following ΔH^o denotes non-ionized vacancies.

Case (1) (O_2 single, O single):

$$\begin{array}{rl} Ni^{2+} + \frac{1}{2}O_2 = O^{2-} + Ni^{3+} + Ni\square^{+} & \Delta H_f^o(s,O_2) \\ O = \frac{1}{2}O_2 & \Delta H^o = -\Delta H_f^o(O) \\ \hline Ni^{2+} + O = O^{2-} + Ni^{3+} + Ni\square^{+} & \Delta H_f^o(s,O) = \Delta H_f^o(s,O_2) - \Delta H_f^o(O) \end{array}$$

Case (2) (O_2 double, O double):

$$\begin{array}{rl} 2Ni^{2+} + \frac{1}{2}O_2 = O^{2-} + 2Ni^{3+} + Ni\square & \Delta H_f^o(d,O_2) \\ O = \frac{1}{2}O_2 & -\Delta H_f^o(O) \\ \hline 2Ni^{2+} + O = O^{2-} + 2Ni^{3+} + Ni\square & \Delta H_f^o(d,O) = \Delta H_f^o(d,O_2) - \Delta H_f^o(O) \end{array}$$

Case (3) (O_2 double, O single):

$$\begin{array}{rl} 2Ni^{2+} + \frac{1}{2}O_2 = O^{2-} + 2Ni^{3+} + Ni\square & \Delta H_f^o(d,O_2) \\ Ni^{3+} + Ni\square = Ni^{2+} + Ni\square^{+} & -\Delta H^o(s \rightarrow d) \\ O = \frac{1}{2}O_2 & -\Delta H_f^o(O) \\ \hline Ni^{2+} + O = O^{2-} + Ni^{3+} + Ni\square^{+} & \Delta H_f^o(s,O) = \Delta H_f^o(d,O_2) - \Delta H^o(s \rightarrow d) - \Delta H_f^o(O) \end{array}$$

Case (4) (O_2 single, O double):

$$\mathrm{Ni^{2+}} + \frac{1}{2}\,\mathrm{O_2} = \mathrm{O^{2-}} + \mathrm{Ni^{3+}} + \mathrm{Ni}\square^{+} \qquad \Delta H_f^o(s,O_2)$$

$$\mathrm{Ni^{2+}} + \mathrm{Ni}\square^{+} = \mathrm{Ni^{3+}} + \mathrm{Ni}\square \qquad \Delta H^o(s \rightarrow d)$$

$$\mathrm{O} = \frac{1}{2}\,\mathrm{O_2} \qquad -\Delta H_f^o(O)$$

$$\mathrm{2Ni^{2+}} + \mathrm{O} = \mathrm{O^{2-}} + \mathrm{2Ni^{3+}} + \mathrm{Ni}\square \qquad \Delta H_f^o(d,O) = \Delta H_f^o(s,O_2) + \Delta H^o(s \rightarrow d) - \Delta H_f^o(O)$$

Case (5) (O_2 double, O non-ionized):

$$\mathrm{2Ni^{2+}} + \frac{1}{2}\,\mathrm{O_2} = \mathrm{O^{2-}} + \mathrm{2Ni^{3+}} + \mathrm{Ni}\square \qquad \Delta H_f^o(d,O_2)$$

$$\mathrm{Ni^{3+}} + \mathrm{Ni}\square = \mathrm{Ni^{2+}} + \mathrm{Ni}\square^{+} \qquad -\Delta H^o(s \rightarrow d)$$

$$\mathrm{Ni^{3+}} + \mathrm{Ni}\square^{+} = \mathrm{Ni^{2+}} + \mathrm{Ni}\square^{++} \qquad -\Delta H^o(n \rightarrow s)$$

$$\mathrm{O} = \frac{1}{2}\,\mathrm{O_2} \qquad -\Delta H_f^o(O)$$

$$\mathrm{O} = \mathrm{O^{2-}} + \mathrm{Ni}\square^{++} \qquad \Delta H_f^o(n,O) = \Delta H_f^o(d,O_2) - \Delta H^o(s \rightarrow d) - \Delta H^o(n \rightarrow s) - \Delta H_f^o(O)$$

Case (6) (O_2 single, O non-ionized):

$$\mathrm{Ni^{2+}} + \frac{1}{2}\,\mathrm{O_2} = \mathrm{O^{2-}} + \mathrm{Ni^{3+}} + \mathrm{Ni}\square^{+} \qquad \Delta H_f^o(s,O_2)$$

$$\mathrm{Ni^{3+}} + \mathrm{Ni}\square^{+} = \mathrm{Ni^{2+}} + \mathrm{Ni}\square^{++} \qquad -\Delta H^o(n \rightarrow s)$$

$$\mathrm{O} = \frac{1}{2}\,\mathrm{O_2} \qquad -\Delta H_f^o(O)$$

$$\mathrm{O} = \mathrm{O^{2-}} + \mathrm{Ni}\square^{++} \qquad \Delta H_f^o(n,O) = \Delta H_f^o(s,O_2) - \Delta H^o(n \rightarrow s) - \Delta H_f^o(O)$$

Now, by methods similar to those used in deriving equation (3), one can show for reaction with atomic oxygen, considering the formation of doubly, singly, and non-ionized vacancies, respectively,

$$\Delta H_O^* = \Delta H_{diff}^* + \frac{1}{3}\,\Delta H_f^o(d,O) \qquad (5)$$

$$\Delta H_O^* = \Delta H_{diff}^* + \frac{1}{2}\,\Delta H_f^o(s,O) \qquad (6)$$

$$\Delta H_O^* = \Delta H_{diff}^* + \Delta H_f^o(n,O) \qquad (7)$$

For the nonequilibrium situation of fixed vacancy concentration case (7), when the temperature is changed, the observed variation in oxidation rate would not reflect a change in vacancy concentrations but would be due only to

a change in diffusion rate resulting from the temperature effect of the Ni diffusion coefficient. Then,

$$\Delta H_0^* = \Delta H_{diff}^* \tag{8}$$

By substituting the appropriate expressions above for $H_f^o(d,0)$, $H_f^o(s,0)$, and $H_f^o(n,0)$ into equations (5), (6), and (7), one then obtains the final expressions for the calculated activation enthalpies for atomic oxygen reaction with Ni for the various possible equilibrium situations:

Case (1):

$$\Delta H_0^* = \Delta H_{diff}^* + \frac{1}{2}\Delta H_f^o(s,O_2) - \frac{1}{2}\Delta H_f^o(0)$$

Case (2):

$$\Delta H_0^* = \Delta H_{diff}^* + \frac{1}{3}\Delta H_f^o(d,O_2) - \frac{1}{3}\Delta H_f^o(0)$$

Case (3):

$$\Delta H_0^* = \Delta H_{diff}^* + \frac{1}{2}\Delta H_f^o(d,O_2) - \frac{1}{2}\Delta H^o(s \rightarrow d) - \frac{1}{2}\Delta H_f^o(0)$$

Case (4):

$$\Delta H_0^* = \Delta H_{diff}^* + \frac{1}{3}\Delta H_f^o(s,O_2) + \frac{1}{3}\Delta H_f^o(s \rightarrow d) - \frac{1}{3}\Delta H_f^o(0)$$

Case (5):

$$\Delta H_0^* = \Delta H_{diff}^* + \Delta H_f^o(d,O_2) - \Delta H^o(s \rightarrow d) - \Delta H^o(n \rightarrow s) - \Delta H_f^o(0)$$

Case (6):

$$\Delta H_0^* = \Delta H_{diff}^* + \Delta H_f^o(s,O_2) - \Delta H^o(n \rightarrow s) - \Delta H_f^o(0)$$

And, by equation (8), for the nonequilibrium situation:

Case (7):

$$\Delta H_0^* = \Delta H_{diff}^*$$

Examination of Vacancy Models

To determine which of the possible cases are consistent with the experimental data and which may be ruled out, the following enthalpies are used:

$$\Delta H_{diff}^* = (26.5 \pm 8) \text{ kcal mole}^{-1}$$

$$\Delta H_f^o(d,O_2) = (58.5 \pm 6) \text{ kcal mole}^{-1}$$

$$\Delta H_f^o(s,O_2) = (39 \pm 4) \text{ kcal mole}^{-1}$$

$$\Delta H_f^o(O) = 60.6 \text{ kcal mole}^{-1}$$

The first three enthalpies were calculated above, while $\Delta H_f^o(O)$ is from the JANAF Thermochemical Tables.[46] $\Delta H^o(s \rightarrow d) = 25$ kcal mole^{-1} (Koel and Gellings[30]). Bauer et al.[38] estimated that $\Delta H^o(n \rightarrow s) = 1/4\ \Delta H^o(s \rightarrow d)$, so $\Delta H^o(n \rightarrow s) = 6.1$ kcal mole^{-1}.

Our observed value for ΔH_0^* is 27 kcal mole^{-1}. The calculated values for the various cases are summarized in table III.

TABLE III.— CALCULATED ACTIVATION ENTHALPIES FOR NiO REACTION

Case	Vacancy types*		ΔH_0^* (calc.), kcal mole^{-1}
	O_2	O	
1	s	s	15.7 ±6
2	d	d	25.8 ±6
3	d	s	13.0 ±7
4	s	d	27.6 ±5
5	d	n	-6.5 ±11
6	s	n	-1.2 ±8.5
7	-	fixed	26.5 ±8

*d, s, and n refer to doubly-ionized, singly-ionized, and non-ionized vacancies, respectively.

The error analysis of equilibrium cases 1 and 2 is made by noting that the first two terms on the right-hand side of the enthalpy equation is, for each case, $\Delta H_{O_2}^* = (46 \pm 6)$ kcal mole^{-1}. For the other equilibrium reactions, the error, ±6 kcal mole^{-1}, is multiplied by the ratio of the sums of the values of the first two terms on the right-hand side of each enthalpy equation to 46. While this may not be strictly correct, it is considered a better estimate of error range than strictly adding individual uncertainties since the values are not independent.

By comparison of the calculated values of ΔH_0^* (table III) with the observed value (27 kcal mole^{-1}), we can immediately rule out the existence of cases 1, 3, 5, and 6. One cannot distinguish, by this analysis, between cases 2, 4, and 7, which are all nearly equal in value.

Saturated Defect Model

Strong support for case 7 is provided by three experimental results from the present study, discussed below: (1) the magnitude of the O reaction rates relative to O_2 rates, (2) the pressure dependence of the reaction rate, and (3) the effect of impurities on the reaction rate.

Comparative reaction rates in O and O_2— For atomic oxygen, one may derive (in a fashion similar to that used for eqs. (1) and (2) for vacancy concentrations in O_2), for the formation of doubly ionized vacancies,

$$[Ni\square]_O = 4^{-1/3}\ P_O^{1/3}\ \exp[-\Delta G_f^o(d,O)/3RT] \qquad (8)$$

Combining equation (8) with (2) and, noting that $\Delta G_c^o = \Delta G_f^o(d,O_2)$, and that the rate is equal to the same constant times the vacancy concentration for O_2 or for O, one may write, for case 2,

$$\frac{\text{Rate O}}{\text{Rate } O_2} = \frac{[Ni\square]_O}{[Ni\square]_{O_2}} = \frac{P_O^{1/3}}{P_{O_2}^{1/6}} \exp[\Delta G_f^o(O)/3RT] \qquad (9)$$

where $\Delta G_f^o(O)$, the standard free energy of formation of atomic oxygen, is $\Delta G_f^o(d,O_2) - \Delta G_f^o(d,O)$. This expression was originally derived by Dickens et al.[29] and allows one to calculate a theoretical ratio of rates.

For case 4, we derive the expression:

$$\frac{\text{Rate O}}{\text{Rate } O_2} = \frac{[Ni\square]_O}{[Ni\square^+]_{O_2}} = \frac{4^{-1/3}P_O^{1/3}}{P_{O_2}^{1/4}} \exp\left[\frac{\frac{1}{2}\Delta G_f^o(s,O_2) - \frac{1}{3}\Delta G_f^o(d,O)}{RT}\right] \qquad (10)$$

The exponential term in this case can only be estimated. Gulbranson and Andrew[19] have calculated a value for $\Delta S_f^o(d,O_2)$ of -7.5 cal deg^{-1} mole^{-1}. By adding ΔS^o for the process $O(g) \rightarrow 1/2\ O_2(g)$, -15.66 cal deg^{-1} mole^{-1}, we obtain a value for $\Delta S_f^o(d,O)$ of -23.2 cal deg^{-1} mole^{-1}. For the formation of a singly ionized cation vacancy, the calculations of Gulbranson and Andrew[19] may be used to yield a value of $\Delta S_f^o(s,O_2)$ = -7.3 cal deg^{-1} mole^{-1}. From the earlier derived values for $\Delta H_f^o(s,O_2)$ (39 ±4 kcal mole^{-1}) and for $\Delta H_f^o(d,O)$ (-2.1 ±6 kcal mole^{-1}), we may then write

$$\Delta G_f^o(s,O_2) = (39{,}000 \pm 4{,}000) + 7.3\ T, \text{ cal mole}^{-1} \qquad (11)$$

and

$$\Delta G_f^o(d,O) = (-2{,}100 \pm 6{,}000) + 23.2\ T, \text{ cal mole}^{-1} \qquad (12)$$

Note that when equations (11) and (12) are combined for use in equation (10), the errors in $\Delta H_f^o(s,O_2)$ and $\Delta H_f^o(d,O)$ are not additive and, in fact, nearly subtract out since they were derived from the same source. A maximum combined error is estimated to be ±1 kcal mole^{-1}. The entropy errors, likewise, nearly cancel. The estimated individual entropy errors are ±0.5 cal deg^{-1} mole^{-1} and the combined errors less than ±0.1 cal deg^{-1} mole^{-1}. This is equivalent to 0.1 kcal mole^{-1} error in G^o at 1100°K and so is neglected relative to the ΔH^o errors in the calculations.

A comparison of the theoretical ratio of oxidation rates in atomic and and molecular oxygen with that observed is given in table IV for the two possible equilibrium cases, 2 and 4. These ratios were determined for the temperature extremes used in the present experiment. For observed rates in molecular oxygen, the data of Douglass et al.[28] were averaged with the high

TABLE IV.— THEORETICAL AND OBSERVED RATIO OF RATES

T,°K	Rate O / Rate O_2 Theoretical Case 2	Rate O / Rate O_2 Theoretical Case 4*	Rate O / Rate O_2 Observed	Theoretical ratio / Observed ratio Case 2	Theoretical ratio / Observed ratio Case 4*
1050	67	130^{+80}_{-49}	30	2.24	4.30 (2.7 to 7.0)
1250	14.4	$27.6^{+13.7}_{-9.1}$	6.25	2.30	4.42 (3.0 to 6.6)

*The ranges are those resulting from the estimated ±1 kcal $mole^{-1}$. uncertainty in the combined free energies of equation (10).

purity data reviewed by Phillips.[44] The value of 46 kcal $mole^{-1}$ determined for $\Delta H^*_{O_2}$ by Douglass et al.[28] is the mean of the values reported in 38-44. The atomic oxygen data for both materials represented in figure 7 were averaged to give representative observed values for that environment.

From this analysis, one can say, with fair certainty, even in light of the estimated theoretical rates, that case 4 (i.e., singly ionized vacancies in O_2 and doubly ionized vacancies in O, both at equilibrium concentrations), which differs significantly from the observed rates, does not appear plausible. The results of the analysis for case 2 (doubly ionized vacancies for both environments), showing a factor of 2.3 variance from the observed, might indicate that this — case 2 — mechanism is not very probable either. However, in view of the range[44] of measured oxidation rates of pure Ni in O_2 by different investigators and the observed importances of sample preparation (surface preparation,[40,45,47,48] annealing[19,49] pre-oxidation[19,47] on the rates, one must admit that this lack of agreement between observed and theoretical ratios does not completely rule out case 2, and, in fact, case 4 may be marginal.

The evidence considered thus far, viz, theoretical activation enthalpies and rates in atomic oxygen, compared with observed values, within the qualifications given in the preceding paragraph, indicates that, while the oxidation of nickel apparently occurs under the influence of near equilibrium concentrations of cation vacancies in O_2, the controlling concentration of vacancies in the presence of atomic oxygen is less (by a factor of 2 or more than the expected equilibrium concentration. Accepting this observation, we hypothesize that the atomic oxygen, at the pressure and temperature conditions of our experiments, with its high thermodynamic potential, causes a saturation of the surface with vacancy defects (i.e., all defect sites are filled) before an

equilibrium concentration can be attained. This model is consistent with the suggestion that the vacancy concentration is constant in our experiments (case 7).[d]

Pressure dependence— In support of the proposed saturated defect model, we observed no dependence of the oxidation rate of nickel on the partial pressure of atomic oxygen under the following inclusive test conditions. First, all the material 1 specimen points in figure 7, which were obtained at partial pressures of atomic oxygen varying from 10 to 16 Nm^{-2}, were extrapolated to a common temperature using the experimentally determined activation enthalpy and the resultant k_p values plotted as a function of P_O (see fig. 8). There was completely random variation of the points in this plot about an average horizontal line which indicated an average error of ±15% and a maximum random error of 29%. These data were obtained for the Ni sample of low purity. Similarly, a study was performed on the high purity Ni, material 2, in which the partial pressure of atomic oxygen varied between 1 and 45 Nm^{-2} (thus, $P_O^{1/3}$ varied by a factor of 3.6) and again the variation of the temperature normalized k_p's fell within experimental error (in this case ±20% maximum). And, lastly, if one includes the results of Dickens et al.,[29] which coincide with our extrapolated values (fig. 7), at their reported pressure of 10^{-3} Nm^{-2} (or if the correction of footnote a is valid, 10^{-1} Nm^{-2}), the oxidation rate is apparently independent of P_O over a range of 10^4 (or 160 if P is 10^{-1} Nm^{-2}). If case 2 or 4 were in effect, a $P_O^{1/3}$ dependence should have been observed (eq. (8)). (For reference, a $P^{1/3}_O$ relationship is indicated on the plot.)

Impurity effect in O and O_2— Perhaps the strongest evidence for the saturated defect model (i.e., case 7 comes from observations regarding the influence of aliovalent impurities on the oxidation rate in atomic oxygen. Just as changes in pressure would be expected to shift the concentration of vacancies at the gas-oxide interface for an equilibrium case, via Le Chatelier's principle, an equilibrium concentration of vacancies should be changed by the introduction of impurities of valence different from 2 (see, e.g., Kofstad[50]). Metal

[d] A comment is required at this point regarding the near constancy with temperature of the theoretical ratio/observed ratio (T/O) for cases 2 and 4 in table II. One might interpret this as indicating that case 2 or 4 is the correct model and that the magnitude at T/O (which should then be unity) is within the range of experimental errors in measuring absolute rates. That is, a constant value of T/O would not normally be expected if the vacancy concentrations were saturated and fixed in atomic oxygen while they varied with temperature in O_2. However, because $\Delta H_f^o(d,O)$ is practically zero (-2.1 ±6) kcal $mole^{-1}$), these two equilibrium models for O would also predict a concentration of vacancies in atomic oxygen which remained nearly constant with temperature changes. (A calculation of $\Delta H_f^o(d,O)$ from the T/O ratios for case 2 at the two temperatures yields a value of 1.2 kcal $mole^{-1}$. Thus, either an equilibrium model with doubly ionized vacancies in atomic oxygen (case 2 or 4) or the saturated defect model is consistent with the observed constancy of T/O.

impurities with valences greater than 2 would be expected to increase the equilibrium concentration of cationic vacancies. As observed by Phillips,[44] in his review of nickel oxidation data, the oxidation rate in O_2 of pure nickel was about 10% that of less pure nickel. Horn[51] also found that small amounts of impurities increased the oxidation rate in O_2 significantly. Apparently, the impurity metals are oxidized rapidly and, in the ionized state, can diffuse to the NiO gas surface to affect the Ni vacancy concentrations.

Most of the present data were obtained with a Ni sample (material 1), which had been represented as being of high purity. Analysis (table I) showed it to contain significant amounts of Mn, Cu, Fe, and Co. Horn[51] specifically observed that small amounts of Mn and Cu in Ni increased its reaction rate with O_2; and Fe (as well as Mn) have been particularly observed to generally increase the rate.[47,52] Cobalt appears to have a smaller effect on the rate.[42,47]

In view of the very large concentrations of foreign metals in material 1, one would predict that the oxidation rate of this material in atomic oxygen should be perhaps a factor of 10 or more higher than that of a very pure sample if equilibrium vacancy concentrations were predominant in controlling the diffusion rate of Ni through NiO. A few measurements were made on a high purity sample ($\leq$ 20 ppm metal impurities, material 2, table I. These parabolic rate constants are shown in figure 7 from which it is seen that the pure sample actually exhibits a slightly higher rate of oxidation by dissociated oxygen (approximately 2.5 times faster than the 98.4% sample). This provides additional evidence that an equilibrium mechanism is inoperative. If the available defect sites of NiO were all occupied in the pure sample, then the addition of impurities, which would have the normal tendency to increase their concentration, would be ineffective in doing so. The observations regarding the impurity effects may thus be taken as strongly supporting a saturated defect model.

Vacancy Calculations for Saturated Defect Model

In molecular oxygen at 0.2 atm and at the two temperature limits of the present experiments (1050° and 1250°K), the equilibrium concentrations of cationic vacancies in NiO is of the order of 10^{-5} and 5×10^{-5} mole fraction,[8,32] respectively. Since the oxidation rate (at a given temperature) is proportional to the number of vacancies (as shown above), the vacancy concentration during the reaction of nickel with atomic oxygen may be estimated. Using the mean oxidation rates found (fig. 7) for both materials purities in atomic oxygen and the mean rate (as calculated earlier) for pure nickel oxidation by molecular oxygen, a vacancy concentration, during oxidation under conditions of the present experiments, of about 5×10^{-4} mole fraction is calculated for both temperatures. (The constant value was expected for either of the allowed cases, case 7 by definition and case 2 and also case 4 by virtue of the fact that $\Delta H_f^o(d,0) \sim 0$.)

Again, using the defect concentration equations of Mitoff[8] and of Tripp and Tallen,[32] the temperature at which the NiO defect concentration reaches

5×10^{-4} in molecular oxygen at $P_{O_2} = 2\times10^4$ Nm^{-2} (0.2 atm - the "normal pressure for oxidation experiments) is calculated to be about 1775°K. At 10^5 Nm^{-2}, it would be approximately 1700°K. These are the temperatures, at the respective O_2 partial pressures, above which one would expect the vacancy sites to become saturated if, in fact, the saturated defect model (i.e., case 7) is correct for the environment of the present studies. Or, conversely, at 1700°K, the vacancy concentration and thus the oxidation rate should become constant at pressures greater than 10^5 Nm^{-2}.

Bauer et al.[38] measured oxidation rates of Ni in O_2 at pressures up to 2 MNm^{-2} between 1275°K and 1475°K. At the higher pressures, above about 5×10^5 Nm^{-2}, their observed rates are apparently constant at all temperatures. Further, it appears that the pressure at which the rate becomes constant may be smaller as the temperature increases. The "break" in their 1475°K data is at approximately 5×10^5 Nm^{-2}. At that temperature and pressure, the vacancy concentration is calculated to be 3×10^{-4}. This is in excellent agreement with the value obtained in the present study, particularly in view of the simplifying assumptions and, more spectacularly, the experimental uncertainties.

One would expect, however, that the high-pressure results of Bauer et al.[38] for O_2 should yield an observed activation enthalpy identical to that observed in the present study, i.e., it should reflect only the vacancy diffusion activation enthalpy. Bauer in fact, did, not observe such a decrease in the activation enthalpy in the high-pressure range. This is not consistent with their observed pressure independence and their model. Note that their statement regarding the closeness of their observed activation enthalpy (50.5 kcal) to that for diffusion of Ni in NiO must be modified to recognize that the measured activation enthalpy for Ni diffusion also includes the term for vacancy formations. Thus, their conclusion regarding the smallness of the enthalpy of vacancy formation is incorrect and they should not have ignored the fact that their Arrhenius slopes were the same in both the low- and high-pressure regions.

Realistically, it is possible to consider that their data do not reflect a clear independence of pressure in the higher range (fig. 2 of Bauer et al.[38]). If this is accepted, the minimum saturation vacancy concentration would have to be greater than that calculated in O_2 at 1475°K and $2MNm^{-2}$, or 3.8×10^{-4}. This value is still consistent with that observed in atomic oxygen.

CONCLUDING REMARKS

By considering the results of past nickel oxidation (and related) studies in molecular oxygen with the present results in atomic oxygen in terms of all possible NiO defect structure combinations in the two environments, the following equilibrium vacancy situations (designated as in Discussion) have been definitively ruled out: (1) singly ionized vacancies forming at equilibrium in O_2 at ordinary pressures and in O in the pressure range of our experiments, (3) doubly ionized vacancies in O_2 and singly ionized vacancies in O, (4) vacancies singly ionized in O_2 and doubly ionized in O, (5) doubly ionized vacancies in O_2 and neutral (non-ionized vacancies in O, and (6) singly ionized

vacancies in O_2 with non-ionized vacancies in O. Except for case 4, these were eliminated on the basis of observed activation enthalpies of reaction compared with theoretical. The third situation appeared not too probable since the observed oxidation rate in atomic oxygen was much smaller (outside of experimental and calculated uncertainties) than the theoretical rate. Additionally, all the evidence cited below, in favor of the saturated defect case, is unfavorable toward this fourth situation, as well as the other two equilibrium cases above.

On the basis of present evidence, two situations are possible: (i) doubly ionized vacancies formed in the presence of O_2 and also in the environment of dissociated oxygen, both at equilibrium concentrations near the surface, and (ii) a saturated and constant concentration of vacancies (of any degree of ionization) formed in the presence of atomic oxygen, irrespective of the situation for O_2. These are both definitely possible on the basis of the observed activation enthalpy of reaction of Ni with O. Observed rates in O and in O_2 and, thus, calculated defect concentrations, provide information that can be interpreted in terms of either model. But the apparent pressure independence of Ni reaction rates with atomic oxygen did indicate that the saturated defect model is the correct one. However, a $P_O^{1/3}$ effect, which would have supported the equilibrium case, is not large compared to experimental uncertainties and therefore the apparent absence of such an effect should not be construed as absolute proof for the saturation of defect sites. Finally, the fact that large concentrations of Mn, Cu, Fe, and Co present as impurities in the nickel did not increase the oxidation rate is quite strong evidence that atomic oxygen at the pressures and temperatures studied creates a saturation of nickel in vacancy defect sites in the NiO film.

The activation enthalpy for reaction of atomic oxygen with nickel appears to be reasonably established, within the limits of error for the theoretical value. The experimental value of 27 kcal $mole^{-1}$ determined from rate measurements on the impure sample, and which agree well with the lower temperature results of Dickens et al.,[29] may be considered as possibly a minimum value when compared with the few data points obtained with the pure material. Yet the maximum possible theoretical value is (26.5 ±8) kcal $mole^{-1}$ and so it is reasonable to expect that the true activation enthalpy lies somewhere within the range of 27 to 34 kcal $mole^{-1}$, the lower limit being more probable.

Additional work should be done, however, on accurate determinations of the reaction rate of pure Ni and, particularly, its oxygen partial pressure dependence, in order to more confidently verify the saturated defect model. Specific attention must be given to sample preparation methods for comparisons of data.

Electrical conductivity measurements, which can normally be performed more precisely than oxidation rate measurements, should be made to determine pressure effects in atomic oxygen. A value for the activation enthalpy for conductance, ΔH_σ^*, in atomic oxygen is predicted to be 5.5 kcal $mole^{-1}$, the same as in molecular oxygen[8] if the saturated defect model is controlling; or ΔH_σ^* (in O_2) + 1/3 $\Delta H_f^o(d,O_2)$ - 1/3 $\Delta H_f^o(O)$ = (4.8 ±2) kcal $mole^{-1}$ if equilibrium doubly ionized vacancies are present in both environments. If singly ionized vacancies are equilibrated in O_2 but doubly ionized vacancies in O (the only

other reasonably possible equilibrium case since others would require a negative ΔH_σ^* in atomic oxygen), the predicted ΔH_σ^* for O is ΔH_σ^* (in O_2) + 1/3 $\Delta H_f^o(s,O_2)$ + 1/3 $\Delta H_f^o(s \rightarrow d)$ - 1/3 $\Delta H_f^o(0)$ or (6.6 ±2) kcal mole^{-1}.

Finally, studies in molecular oxygen (oxidation of Ni or conductivity of NiO) should be extended to high pressures and temperatures to attempt saturation of defect sites to test the predictions resulting from the atomic oxygen data. Measurements in atomic oxygen should be extended to as low pressures as possible so that verified equilibrium concentrations of vacancies can be determined. (Temperature should have little effect since $\Delta H_f^o(d,O) \simeq 0$.) Then it could be shown conclusively which degrees of vacancy ionization occur in O_2 and in O.

REFERENCES

1. Wagner, C.: "Beitrag zur Theorie des Anlaufrorganges III," Z. Phys. Chem., Vol. 34, 1938, pp. 455-475.

2. von Baumbach, H. H.; and Wagner, C.: "Die elektrische Leitfährgkeit von Nickeloxyd," Z. Phys. Chem., Vol. 24, 1934, pp. 59-62.

3. Verway, E. J.; Haaijman, P. W.; Romeijn, F. C.; and Van Oosterhout, G. W.: "Controlled-Valancy Semiconductors,: Phillips Research Reports, Vol. 5, 1950, pp. 173-187.

4. Fueki, K.; and Wagner, J. B., Jr.: "Studies of the Oxidation of Nickel in the Temperature Range of 900° to 1400°C," J. Electrochem. Soc., Vol. 112, No. 4, 1965, pp. 384-388.

5. Kubaschewski, O.; and Hopkins, B. B.: Oxidation of Metals and Alloys. Butterworths, London, 1962, pp. 20-23.

6. Eror, N. G.; and Wagner, J. B., Jr.: "Electrical Conductivity of Single Crystalline Nickel Oxide," Phys. Stat. Sol., Vol. 35, No. 2, 1969, pp. 641-51.

7. Uno, R.: "Electrical Conduction of NiO at High Temperature." J. Phys. Soc. Japan, Vol. 22, 1967, pp. 1502-7.

8. Mitoff, S. P.: "Electrical Conductivity and Thermodynamic Equilibrium in Nickel Oxide," J. Chem. Phys., Vol. 35, No. 3, 1961, pp. 882-889.

9. Pizzini, S.; and Morlotti, R.: "Thermodynamic and Transport Properties of Stoichiometric and Non-Stoichiometric Nickel Oxide," J. Electrochem. Soc., Vol. 114, No. 11, 1967, pp. 1179-89.

10. Meier, G. H.; and Rapp, R. A.: "Electrical Conductivities and Defect Structures of Pure NiO and Chromium-Doped NiO," Z. Phys. Chem. N.F., Vol. 74, 1971, pp. 168-189.

11. Fehsenfeld, F. C.; Evenson, K. M.; and Brioda, H. P.: "Microwave Discharge Cavities Operating at 2450 MHz," Rev. Sci. Instr., Vol. 36, No. 3, 1965, pp. 294-298.

12. Brandenberger, J. R.: "Regulated Microwave Power Supply for Excitation of Electrodeless Lamps," Rev. Sci. Instr., Vol. 41, 1970, pp. 1535-1537.

13. Kaufman, F.: "The Air Afterglow and Its Use in the Study of Some Reactions of Atomic Oxygen," Proc. Roy. Soc., Vol. A247, 1958, pp. 123-139.

14. Kaufman, F.: "Air Afterglow and Kinetics of Some Reactions of Atomic Oxygen," J. Chem. Phys., Vol. 28, 1958, pp. 352-353.

15. Kaufman, F.: "Reactions of Oxygen Atoms," Progress in Reaction Kinetics, G. Porter, ed., Pergamon Press, New York, 1961, pp. 8-10.

16. Barton, A. F.: "Gas Flow Meters for Small Rates of Flow,: Ind. Eng. Chem., Vol. 11, 1919, pp. 623-629.

17. Hauffe, K.; Pethe, L.; Schmidt, R.; and Morrison, S. R.: "On the Mechanism of Formation of Thin Oxide Layers on Nickel," J. Electrochem. Soc., Vol. 115, No. 5, 1968, pp. 456-461.

18. Engell, H. H.; Hauffe, K.; and Ilschner, B.: "Uber die Kinetik der Oxydation von Nickel bei 400°C," Z. f. Electrochem.; Vol. 58, No. 7, 1954, pp. 478-482.

19. Gulbranson, E. A.; and Andrew, K. F.: "The Kinetics of Oxidation of High Purity Nickel," J. Electrochem. Soc., Vol. 101, No. 3, 1954, pp. 128-140.

20. Wagner, C.: "Dissociation of Molecular O_2 as the Rate Determining Step During the Initial Stage of the Oxidation of Ni at 250°C," Corrosion Sci., Vol. 10, pp. 641-647.

21. Graham, M. J.; and Cohen, M.: "On the Mechanism of Low-Temperature Oxidation (23°-450°C) of Polycrystalline Nickel," J. Electrochem. Soc.-Solid-State Sci. Tech., Vol. 119, 1972, pp. 879-882.

22. Hales, R.; Hill, A. C.; and Wild, R. K.: "The Oxidation of Nickel at Reduced Pressures," Corrosion Sci., Vol. 13, 1973, pp. 325-336.

23. Perrow, J. M.; Smeltzer, W. W.; and Ham, R. K.: "On the Nature of Short-Circuit Diffusion Paths in Nickel Oxide Films," Acta Met., Vol. 15, 1967, pp. 577-579.

24. Perrow, J. M.; Smeltzer, W. W.; and Embury, J. D.: "The Role of Structural Defects in the Growth of Nickel Oxide Films," Acta Met., Vol. 16, 1968, pp. 1209-1218.

25. Kroger, F. A.: The Chemistry of Imperfect Crystals, North Holland, Amsterdam, 1964.

26. Wagner, C.: "Theory of the Tarnishing Process," Z. Phys. Chem., Vol. 21, 1933, pp. 25-41.

27. Wagner, C.: Theory of the Tarnishing Process II," Z. Phys. Chem.; Vol. 32, 1936, pp. 447-462.

28. Douglass, D. L.; Kumar, A.; and Nasrallah, M.: "The Development of Oxidation Resistant Alloys for High Temperature Structual Use," UCLA-ENG-7260, Aug. 1972.

29. Dickens, P. G.; Heckingbottom, R.; and Linnett, J. W.: "Oxidation of Metals and Alloys — Part II — Oxidation of Metals by Atomic and Molecular Oxygen," Trans. Far. Soc., Vol. 65, 1969, pp. 2235-2247.

30. Koel, G. J.; and Gellings P. J.: "The Contribution of Different Types of Point Defects to Diffusion in CoO and NiO during Oxidation of the Metals," Oxid. Metals, Vol. 5, No. 3, 1972, pp. 185-199.

31. Reijnen, P.: "Non-Stoichiometry and Sintering of Impure Solids," in Reactivity of Solids, Proc. 6th Intern. Symp., Schenectady, N. Y. 1968 pp. 99-112.

32. Tripp, W. C.; and Tallan, N. M.: "Gravimetric Determination of Defect Concentrations in NiO," J. Amer. Cer. Soc., Vol. 53, No. 10, 1970, pp. 531-533.

33. Lindner, R.: "Some Problems of Solid State Chemistry with Special Regard to Diffusion and Reaction in Oxide Systems," Proc. 10th Solvay Conf., Brussels, 1956, pp. 459-469.

34. Lindner, R.: "Radioactive Methods of Solid State Chemistry," 3rd Intern. Meeting on the Reactivity of Solids, Madrid, 1956, pp. 509-520.

35. Lindner, R.; and Akerstrom, A.: "Diffusion of Nickel-63 in NiO," Disc. Faraday Soc., Vol. 23, 1957, pp. 133-136.

36. Shim, N.; and Moore, W.: "Diffusion of Nickel in Nickel Oxide," J. Chem. Phys., Vol. 26, No. 4, 1957, pp. 802-804.

37. Tretyakov, Y. D.; and Rapp, R. A.: "Nonstoichiometric and Defect Structures in Pure Nickel Oxide and Lithium Ferrite," Trans. AIME, Vol. 245, 1969, pp. 1235-1241.

38. Bauer, J. P.; Bartlett, R. W.; Ong, J. R., Jr.; and Fassell, W. M., Jr.: "High Pressure Oxidation of Metals, Nickel in Oxygen," J. Electrochem. Soc., Vol. 110, No. 3, 1963, pp. 185-189.

39. Sartell, J. A.; and Li, C. H.: "The Mechanism of Oxidation of High Purity Nickel in the Range 950-1200°C," J. Inst. Metals, Vol. 90, 1961, pp. 92-96.

40. Gulbranson, E. A.; and Andrew, K. F.: "High Temperature Oxidation of High Purity Nickel between 750° and 1050°C," J. Electrochem. Soc., Vol. 104, No. 7, 1957, pp. 451-454.

41. Berry, L.; and Paipassi, J.: "Sar la Cinetique de L'oxydation du Nickel dans l'air aux Temperatures Elevees," Compt. Rand., Vol. 255, 1962, pp. 2253-2255.

42. Frederick, S. F.; and Cornet, I.: "The Effect of Cobalt on the High Temperature Oxidation of Nickel," J. Electrochem. Soc., Vol. 102, No. 6, 1955, pp. 285-291.

43. Zima, G. E.: "Some High Temperature Oxidation Characteristics of Nickel with Chromium Additions," Trans. Amer. Soc. Mat., Vol. 49, 1957, pp. 924-947.

44. Phillips, W. L., Jr.: "Oxidation Rates of Pure and Less Pure Nickel," J. Electrochem. Soc., Vol. 110, No. 9, 1963, pp 1014-1015.

45. Graham, M. J.; Sproule, G. I.; Caplan, D.; and Cohen, M.: "The Effect of Surface Preparation on the Oxidation of Nickel," J. Electrochem. Soc.-Solid-State Sci. Tech., Vol. 119, No. 7, 1972, pp. 883-887.

46. Stull, D. R.; and Prophet, H.: JANAF Thermochemical Tables, 2nd ed., NSRDS-NBS 37, 1971.

47. Wood, G. C.; Wright, I. C.; and Ferguson, J. M.: "The Oxidation of Ni and Co and of Ni/Co Alloys at High Temperatures," Corrosion Sci., Vol. 5, 1965, pp. 645-661.

48. Gulbranson, E. A.; and Andrew, K. F.: "High Temperature Oxidation of High Purity Nickel Between 750° and 1550°C," J. Electrochem. Soc., Vol. 105, 1958, pp. 363-364.

49. Caplan, D.; Graham, M. J.; and Cohen, M.: "Effect of Cold Work on the Oxidation of Nickel at High Temperature," J. Electrochem. Soc.-Solid-State Sci. Tech., Vol. 119, No. 9, 1972, pp. 1205-1215.

50. Kofstad, P.: Nonstoichiometry, Diffusion, and Electrical Conductivity in Binary Oxides, Wiley, Interscience, N.Y. 1972, pp. 20-21.

51. Horn, L.: "The Effect of Addition Elements on the Oxidation of Nickel and Chromium-Nickel Alloys," Z. Metallk., Vol. 40, 1949, pp. 73-76.

52. Van Don Brock, J. J.; and Meijering, J. L.: "Kinetics of the Oxidation of Nickel and Some of Its Alloys," Acta Met., Vol. 76, 1968, pp. 375-379.

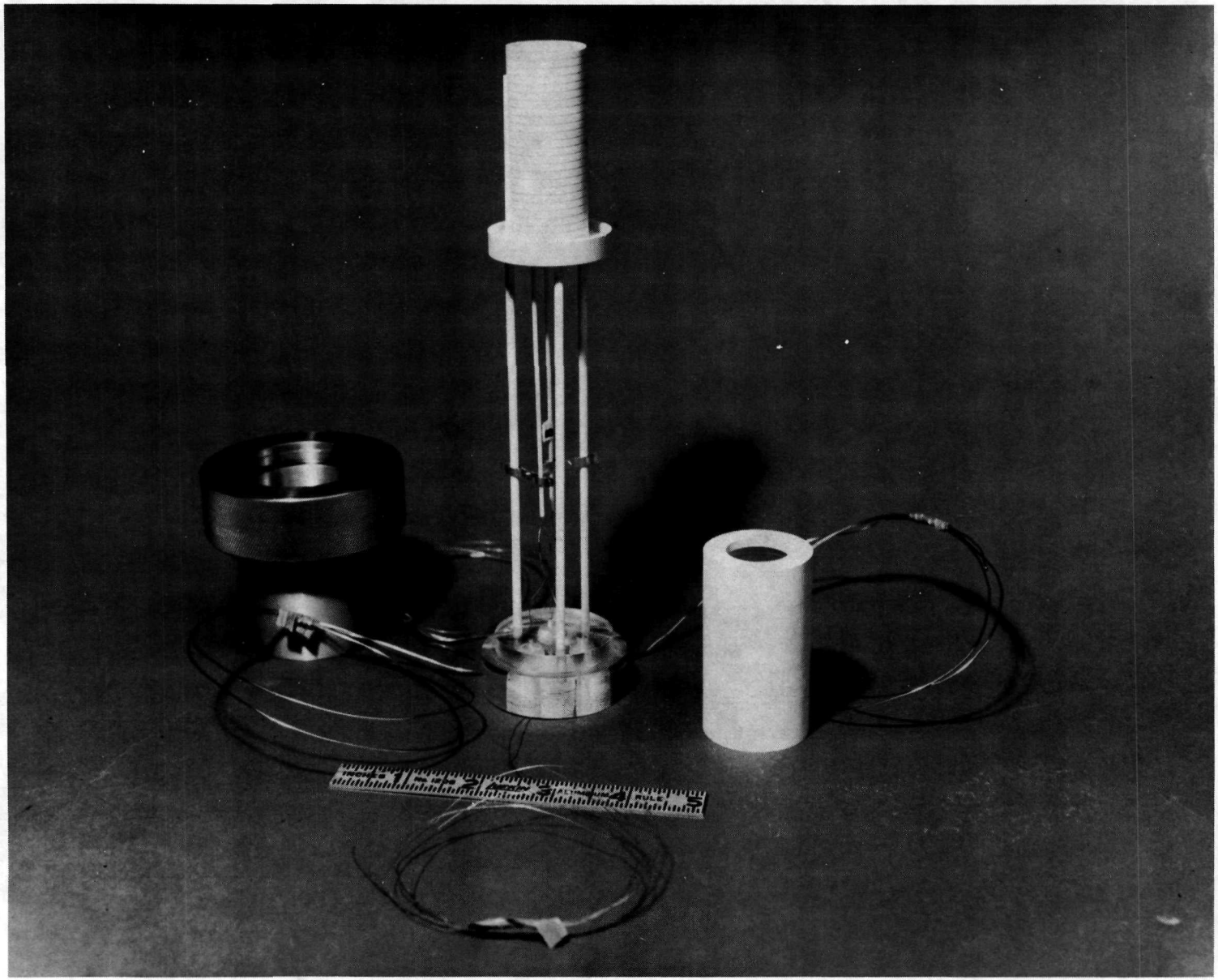

Figure 1.— Disassembled view of reaction furnace.

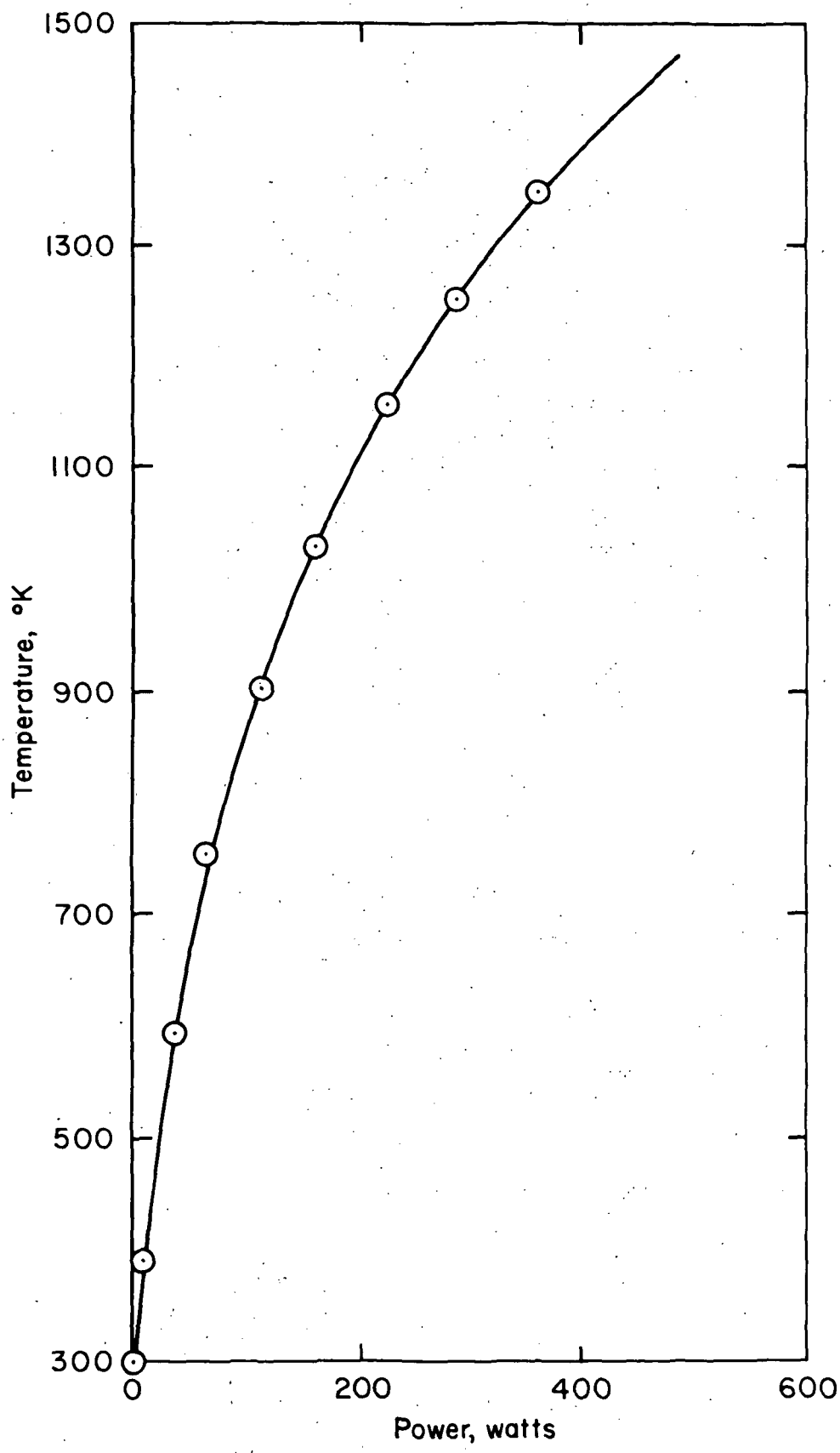

Figure 2.– Steady-state power requirements of furnace.

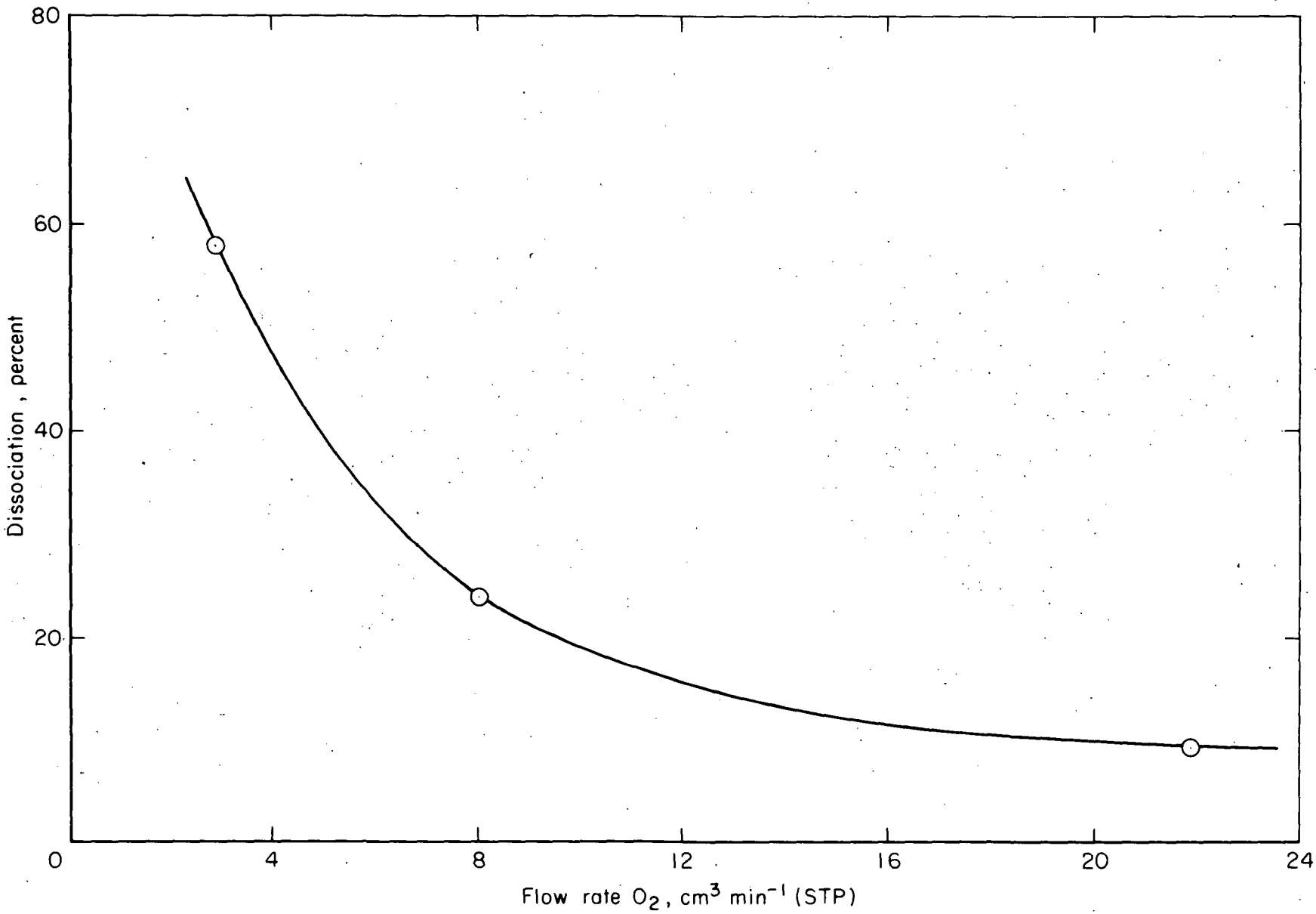

Figure 3.— Effect of flow rate on percent dissociation of oxygen. Conditions: Ni sample in furnace; 80% microwave power; all discharge in furnace; $P^o_{O_2}$ = 15 Nm^{-2}; T = 1075°K.

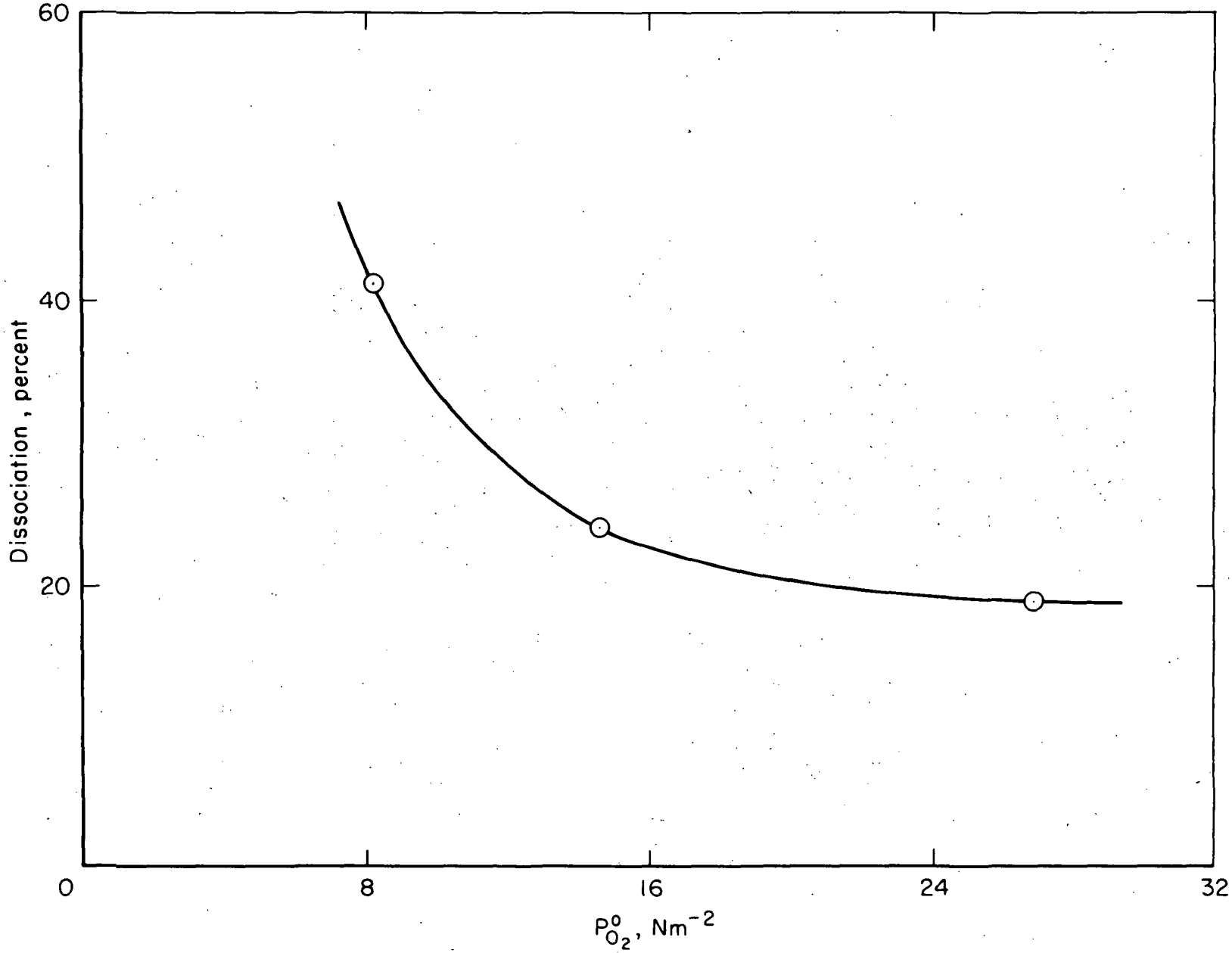

Figure.4.— Effect of pressure on percent dissociation of oxygen. Conditions: Ni sample in furnace; 80% microwave power; all discharge in furnace; flow rate = 8.0 $cm^3 min^{-1}$ (STP); T = 1075°K.

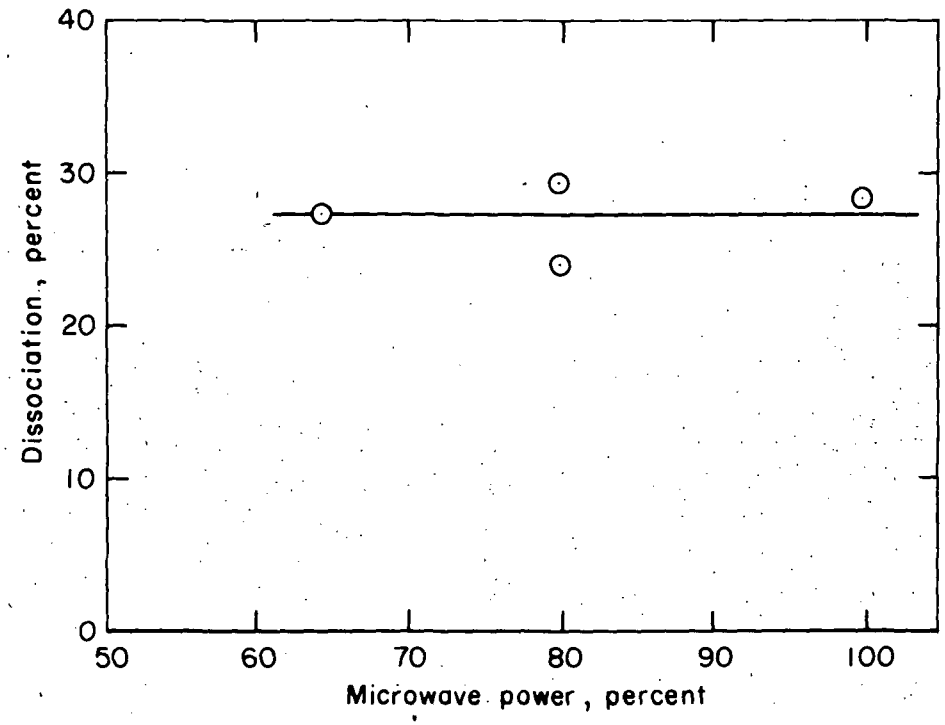

Figure 5.— Effect of microwave power on percent dissociation of oxygen; 100% power ≈ 100 W. Conditions: Ni sample in furnace; all discharge in furnace; $P^{o}_{O_2}$ = 15 Nm^{-2}; flow rate = 8.0 cm^3min^{-1} (STP); T = 1075°K.

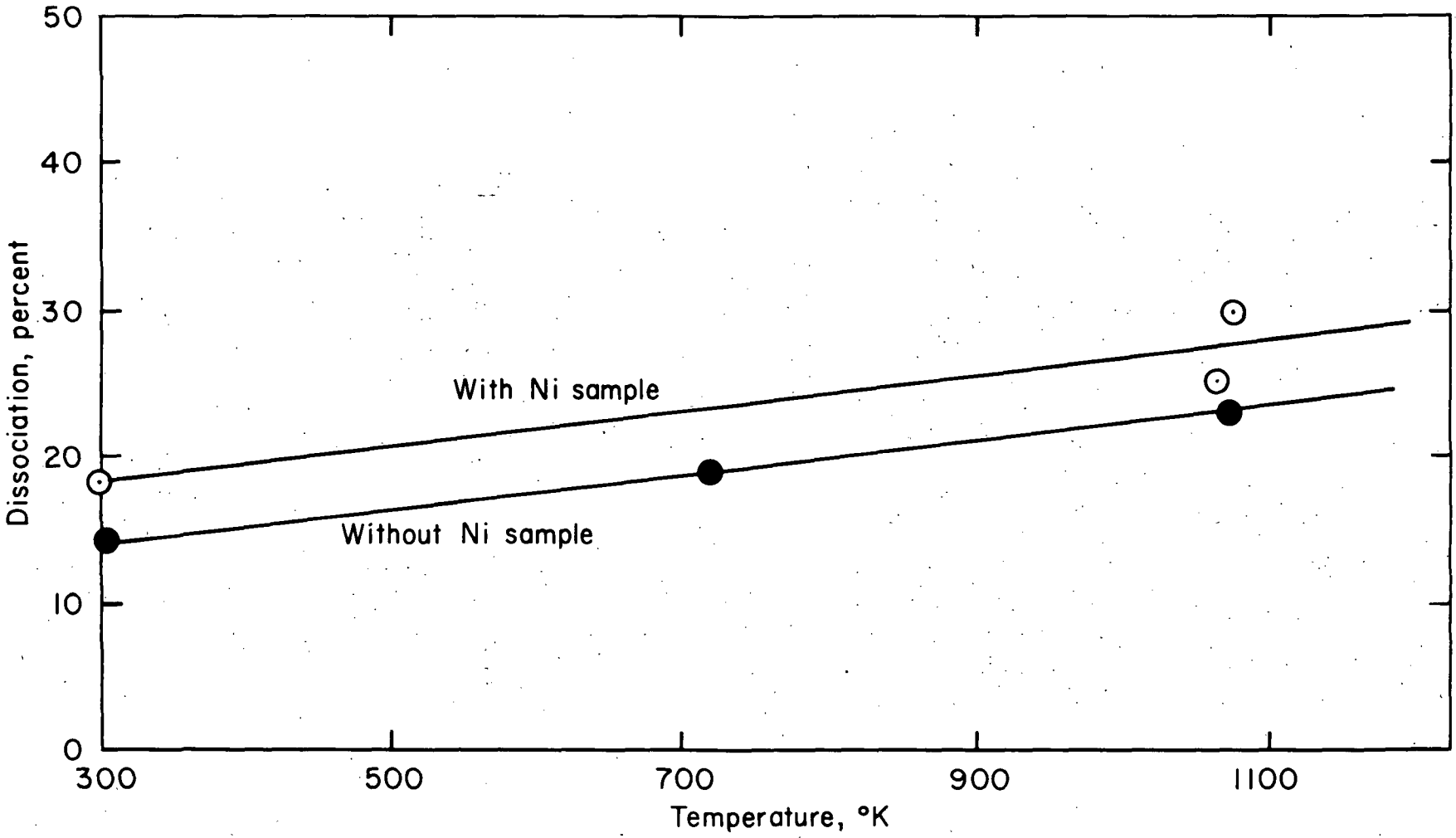

Figure 6.— Effect of temperature on percent dissociation of oxygen. Conditions: 80% microwave power; all discharge in furnace; $P^{o}_{O_2}$ = 15 Nm^{-2}; flow rate = 8.0 $cm^3 min^{-1}$ (STP).

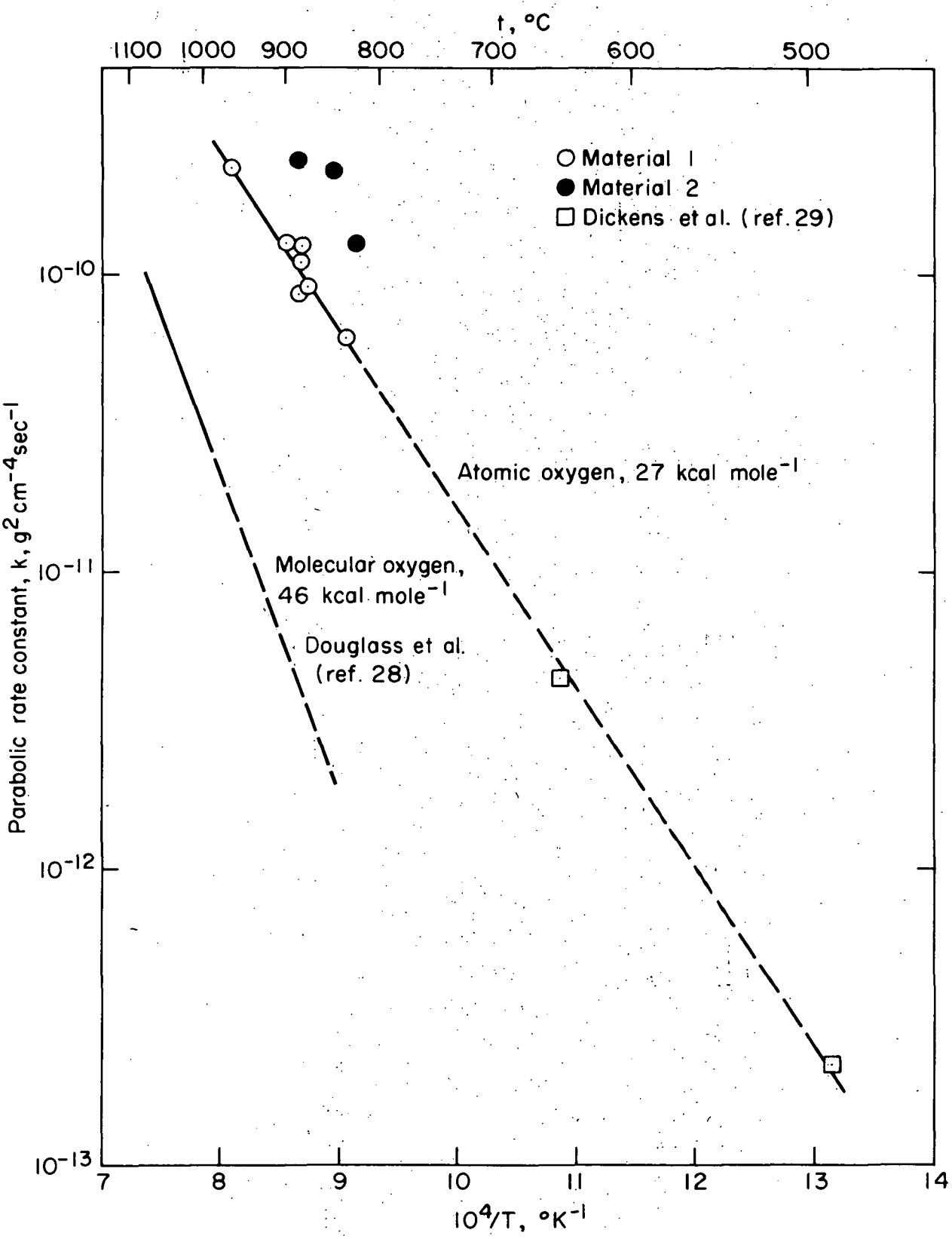

Figure 7.— Arrhenius plots for nickel reaction with atomic and molecular oxygen.

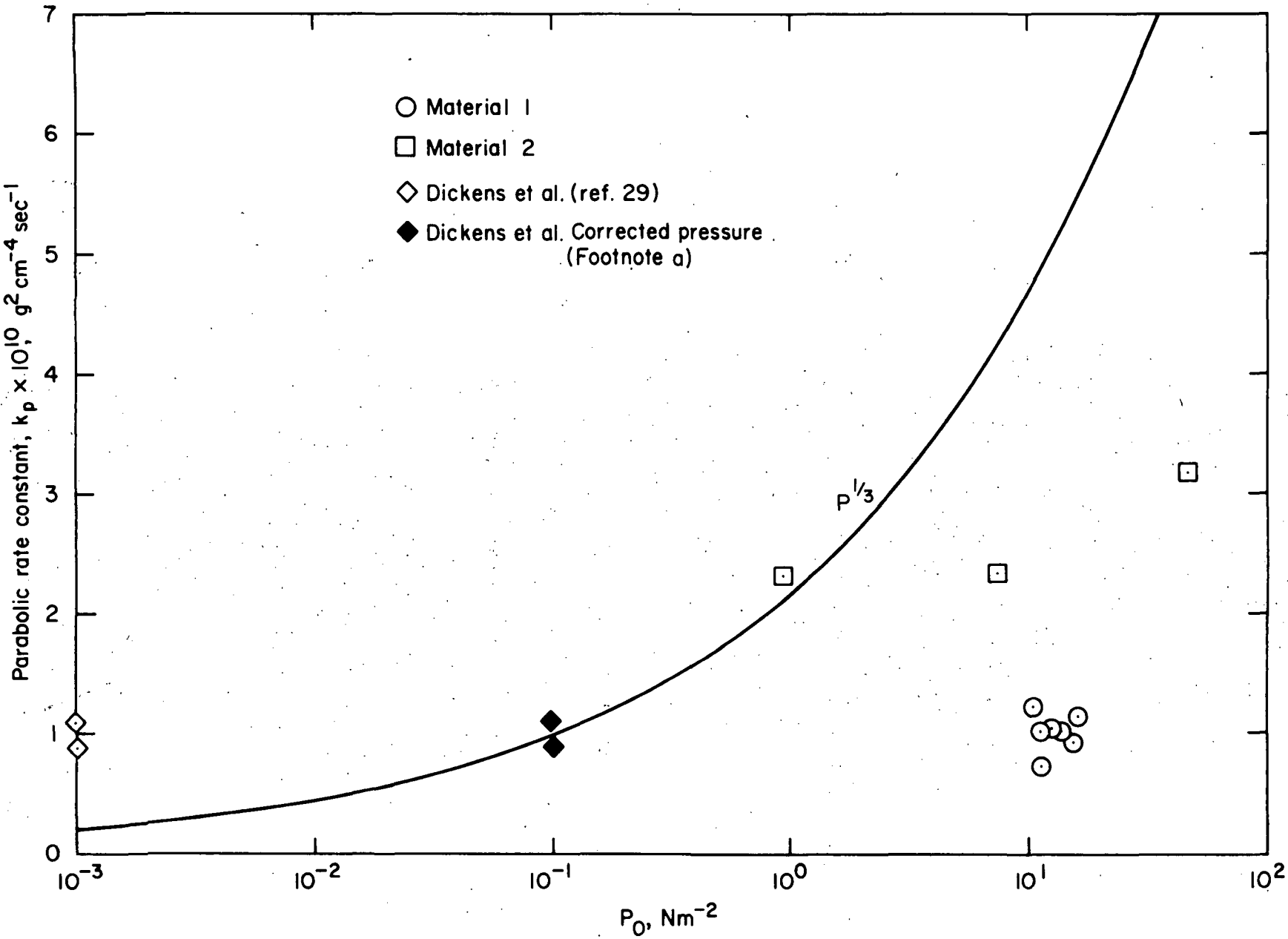

Figure 8.— Pressure dependence of parabolic rate constant for atomic oxygen reaction with nickel; all rates extrapolated to 1152°K.